

Non-Smooth Dynamics in the Stommel Model

With a Subtitle

by

Cody Griffith & Rachel Kuske

B.Sc., Metropolitan State University of Denver, 2016

A THESIS SUBMITTED IN PARTIAL FULFILLMENT OF
THE REQUIREMENTS FOR THE DEGREE OF

MASTER OF SCIENCE

in

The Faculty of Graduate and Postdoctoral Studies

(Mathematics)

THE UNIVERSITY OF BRITISH COLUMBIA

(Vancouver)

July 2017

© Cody Griffith & Rachel Kuske ??

Abstract

Abstract

Lay Summary

Lay Summary

Introduction

MAIN RESULT: Non-smooth bifurcations are a topic that arise in special systems and for how frequent they appear, they have not been analyzed nearly as much as their smooth counter parts. This paper will discuss pinpointing the tipping behavior in the classic Stommel model around the non-smooth bifurcation as well as generalize the canonical system. First an analysis on a simpler one dimensional topologically equivalent system provides insight into approaching the full two dimensional Stommel model.

Background

Stommel Model

([1] [6] [7] [8] are all good references on the climate change focus by the THC)

Global circulation models have primarily focused on three different categories:

- Atmospheric- the effect of greenhouse gases have on the atmosphere,
- Oceanic- the effect of tides and interaction of temperature and salinity on the ocean,
- Sea ice and land surface components.

These categories all contribute significantly to the overall prediction of weather and climate for the planet, which has importance to just about every industry and economy. Failure to adhere to and prepare for sudden changes in the climate led to drastic situations like the drought that led to the great dust bowl. Atmospheric models have been vastly studied but far less work has been done on the contribution from the ocean and the dynamics that drive the tides and current.

As such the oceanic patterns around regions of bi-stability where differing temperature and salinity, also known as the thermohaline circulation (THC), can cause abrupt qualitative changes, Henry Stommel proposed the two box model in 1961, see figure 1. In [9], Stommel suggests that there are actually two different stability regimes in the system that he has suggested and concluded that the oceanic dynamics behave very similarly about these equilibria. These type of systems have since been a heavily studied area for both climatology due to the wide ranging applications and dynamical systems for its generalization into dual stability.

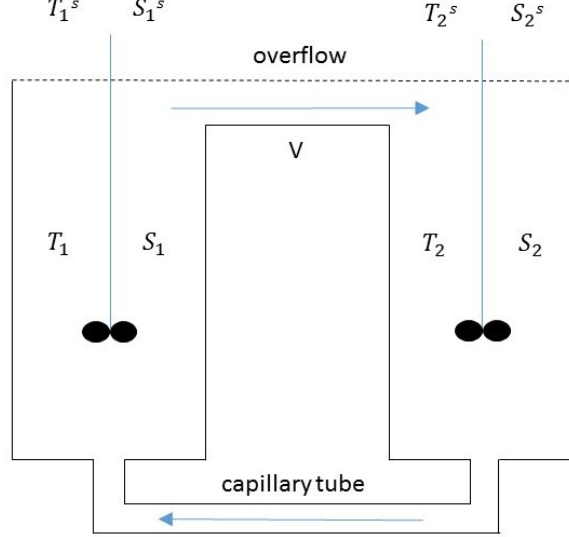


Figure 1: The Stommel Two Box Model: Differing volume boxes with a temperature and salinity T_i and S_i . The boxes are connected by an overflow and capillary tube that has a flow V . There is also a surface temperature and salinity for each box T_i^s and S_i^s . We also assume well mixing occurs.

With emphasis on mathematics, the focus of this paper will be on developing an effective approach to warrant an accurate solution and thus the physical quantities are brushed aside in favor of their non-dimensional alternatives. In the non-dimensionalized Stommel Model, we consider the system

$$\begin{aligned}\frac{dT}{dt} &= \eta_1 - T(1 + |T - S|), \\ \frac{dS}{dt} &= \eta_2 - S(\eta_3 + |T - S|),\end{aligned}\tag{1}$$

where the variables T, S are the temperature and salinity respectively. The parameters η_1, η_2 , and η_3 are all dimensionless quantities that all have physical interpretation to the relaxation times and volumes of the box. Where η_1 can be thought of as the thermal variation, η_2 as the saline variation, and η_3 as the ratio of relaxation times of temperature and salinity. η_1 is a positive quantity that can take any value whereas η_3 is also positive but has

the unique ability to determine the orientation of equilibrium. A standard orientation will be when $\eta_3 < 1$, $\eta_3 = 1$ is a special case and $\eta_3 > 1$ will have reverse orientation, this can be seen in figure 3.

The parameter η_2 turns out to be the most interesting as different values can cause major qualitative and quantitative changes in the dynamics of the system. These changes have been discovered at two different points in the system, each being called either a smooth or a non-smooth saddle-node bifurcation.

It is convenient to view this system in terms of the variable $V = T - S$, which leads to the system,

$$\begin{aligned}\frac{dT}{dt} &= \eta_1 - T(1 + |T - S|), \\ \frac{dV}{dt} &= (\eta_1 - \eta_2) - V|V| - T + \eta_3(T - V).\end{aligned}\tag{2}$$

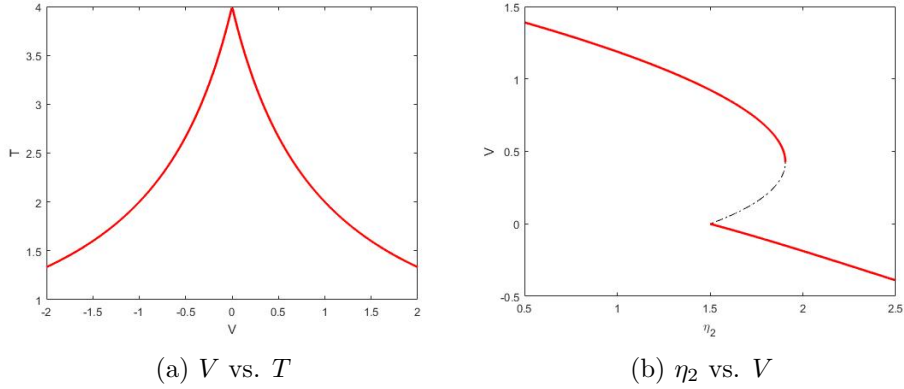


Figure 2: The equilibria of the non-dimensionalized system (2) with $\eta_1 = 4$ and $\eta_3 = .375$. We can see non-smooth behavior happening in both plots when $V = 0$. The red line indicates a stable branch where the dashed dotted line is for an unstable branch.

As shown in figure 2, the equilibrium curves reveal much about the dynamics. In (a) the graph of equilibria for V vs. T shows non-smooth behavior occurring at $V = 0$ and in (b) the two types of bifurcation appear clearly in the graph of equilibria for η_2 vs. V . The location of the non-smooth bifurcation can be found analytically, $\eta_2 = \eta_1 \eta_3$, and the smooth bifurcation is the only real solution to a cubic polynomial. In this plot, both the upper and lower branches of the equilibrium are stable with the middle branch being

unstable. The smoothness of each bifurcation is apparent and arise from the absolute value term in the defining dynamics of (2), which is non-smooth only at $V = 0$.

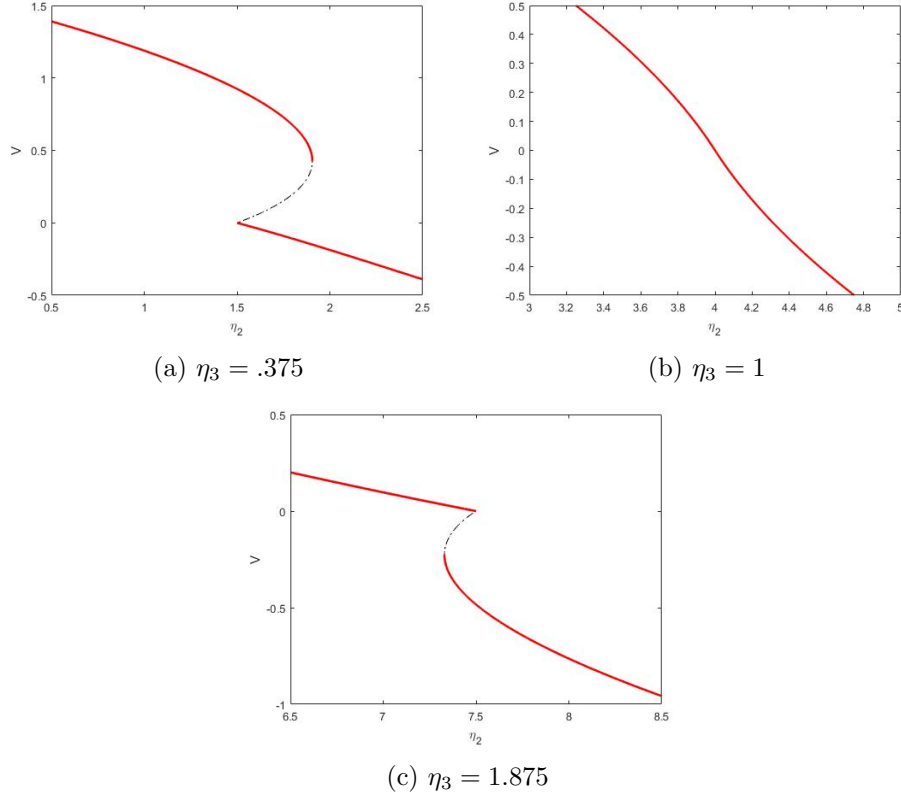


Figure 3: The choice in η_3 turns out to dictate the orientation of the problem, in each plot we have fixed $\eta_1 = 4$. The case for $\eta_3 = 1$ is special due to the two bifurcations overlap and

Much is known about the Stommel model in the case where η_2 is fixed to be a constant value throughout the analysis but realistically this is not the case. In [7] this parameter is described as the influx of freshwater into the Atlantic and the change in this parameter is justified by a positive feedback loop for salinity that drives the THC to move high-salinity water towards deep oceans. This loop causes the abrupt smooth bifurcation but then afterwards, a salinity deficit causes the parameter to decrease back towards the non-smooth bifurcation. In both the smooth and non-smooth case, we see the bifurcation parameter having the ability to vary over time. (MAYBE OMIT)

The parameter changing very slowly is where the focus of this paper lies. A system with a parameter known to cause a bifurcation will no longer admit a bifurcation in the standard sense when there is slow variation. Instead, these conditions give rise to a smooth but rapid change in the system equilibria and where this occurs is called a tipping point.

Slowly Varying Tipping

A tipping point is a point that causes an abrupt transition in dynamical behavior as the system moves into a qualitatively different state. The idea being that some positive feedback pushes change towards this different state once a critical point has been passed, for example in biological systems [2]. These are known to be caused by small changes in one or more parameters in the system. An analysis that considers a multitude of mechanisms interacting with tipping can be found in [10].

Tipping points have been discovered to occur in a wide variety of systems and have become a big staple in the study of areas like catastrophe theory. They can aid in predicting the future of a system and even be a warning for irreversible change like in the case of the Stommel model. A tipping point thus shares similar characteristics of a bifurcation and may or may not occur close to the standard bifurcation location.

The task of finding where tipping occurs depends on the situation, but in general the approach is to search for when a solution to a problem fails or becomes uncontrollable. This can happen, for example, when the interior of a square root becomes negative or when an exponential grows too quickly, both of which we see throughout this paper.

One Dimensional Model

We consider a system that is topologically equivalent to the more complex two dimensional Stommel model,

$$\begin{aligned} \frac{dx}{dt} &= -\mu + 2|x| - x|x| + A \sin(\Omega t), & \frac{d\mu}{dt} &= -\epsilon, & 0 < \epsilon \ll 1, \\ x(0) &= x_i, & \mu(0) &= \mu_i, \end{aligned} \quad (3)$$

where the constants used are the drift rate ϵ , the amplitude of oscillation A and the frequency Ω .

The system (3) is generalized from a basic model that contains both a smooth and non-smooth saddle-node bifurcation. This type of behavior gives the

topological equivalence to the Stommel model and hence good reason to test generalization like slow variation or oscillatory forcing. In each case, emphasis is put on the non-smooth component of the model to give further insight into the Stommel model.

Static μ and Bifurcations

Consider the system (3) with $A = 0$ and $\epsilon = 0$, which is our basic system with a static μ and no forcing. Setting the system equal to zero, we find there are two stable equilibrium branches. Denote these x_l and x_u for lower and upper respectfully, and a single unstable branch, x_{un} ,

$$x_l = 1 - \sqrt{1 + \mu}, \quad x_u = 1 + \sqrt{1 - \mu}, \quad x_{un} = 1 - \sqrt{1 - \mu},$$

where x_l is valid for $\mu \geq 0$ and x_u, x_{un} for $\mu \leq 1$. Thus this system always has a stable equilibrium for every choice in the parameter, but has a region of bi-stability for $0 \leq \mu \leq 1$. This indicates that both edges of this region are bifurcations, $\mu = 0$ and $\mu = 1$, as they cause shifts in stability. Upon further inspection, the points $(x, \mu) = (0, 0)$ and $(x, \mu) = (1, 1)$ are non-smooth and smooth saddle-node bifurcations respectfully. All of this can be seen in figure 4.

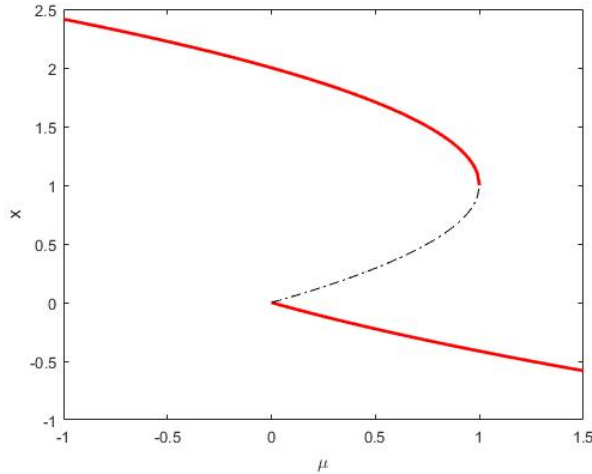


Figure 4: This is the one-dimensional bifurcation diagram and we see the upper and lower equilibrium branches as well as the unstable branch. The non-smooth bifurcation occurs at $(0,0)$ and the smooth bifurcation occurs at $(1,1)$. Both of which are saddle-nodes due to the annihilating equilibria.

Slowly varying μ

Consider (3) with $A = 0$ and $\epsilon > 0$. Here the parameter is allowed to change slowly and thus a bifurcation no longer occurs. Instead, it should be expected that a tipping point occurs nearby the previous bifurcation points. The smooth case is well understood (see Zhu & Kuske [10]), so let us consider an approach towards discovering the non-smooth tipping point. To do so we begin by allowing the initial conditions to be on the lower equilibrium branch, $x_i = 1 - \sqrt{1 + \mu_i}$ and $\mu_i > 0$. Now our calculations will be centered around the stable lower branch and have emphasis on $x < 0$. Since the parameter μ is a slow component to the overall problem, it makes sense to consider a rescaling approach where we use slow time, $t = \epsilon\tau$, with $x < 0$. With this in mind, the system (3) becomes

$$\epsilon \frac{dx}{d\tau} = -\mu - 2x + x^2, \quad \frac{d\mu}{d\tau} = -1. \quad (4)$$

At this point, we adopt the common practice of using an asymptotic expansion in terms of the present small quantity ϵ ,

$$x \sim x_0 + \epsilon x_1 + \epsilon^2 x_2 + O(\epsilon^3). \quad (5)$$

This expansion will capture the slow variable's contribution to a solution while sorting the components by magnitude. Thus, substituting (5) into (4), we get the following system of equations.

$$\begin{aligned} O(1): \quad 0 &= -\mu - 2x_0 + x_0^2 \Rightarrow & x_0 &= 1 - \sqrt{1 + \mu}, \\ O(\epsilon): \quad x_{0\tau} &= -2x_1 + 2x_1x_0 \Rightarrow & x_1 &= \frac{1}{4(1 + \mu)}, \\ O(\epsilon^2): \quad x_{1\tau} &= -2x_2 + 2x_0x_2 + x_1^2 \Rightarrow & x_2 &= \frac{-3}{32(1 + \mu)^{5/2}}. \end{aligned}$$

Thus, (5) becomes

$$x \sim 1 - \sqrt{1 + \mu} + \epsilon \frac{1}{4(1 + \mu)} - \epsilon^2 \frac{3}{32(1 + \mu)^{5/2}} + O(\epsilon^3). \quad (6)$$

But as the dynamics of x in (3) change at $x = 0$ due to the absolute value, this solution is valid only for $x < 0$ and $\mu > 0$. This gives rise to a critical point at $(x_c, \mu_c) = (0, 0)$ which is the non-smooth bifurcation, and a local analysis about this point is necessary.

Time has already been scaled but now scaling our spatial variable is a must to conduct the local analysis. To find this scaling, we look for when the terms in (6) begin to reorder, and this happens when $\mu \sim O(\epsilon)$. At the same time, we notice that when μ is on this order, $x \sim O(\epsilon)$. This implies that both the parameter and the spatial variable must be scaled by ϵ , thus let $x = \epsilon z$ and $\mu = \epsilon m$. From this our system (3) becomes,

$$\frac{dz}{dt} = -m + 2z - \epsilon z^2, \quad \frac{dm}{dt} = -1. \quad (7)$$

Another common method to capture the interacting dynamics between the system and the parameter is to change the time variable to be in terms of the parameter using the chain rule from differential calculus. Introducing this into our approach, we get a system that we can find it's leading order solution to,

$$\begin{aligned} \frac{dz}{dt} &= \frac{dz}{dm} \frac{dm}{dt}, \\ \frac{dz}{dm} &= m - 2z + \epsilon z^2, \\ z(m) &= C e^{-2m} + \frac{m}{2} - \frac{1}{4} + O(\epsilon). \end{aligned}$$

Finally writing this in terms of the original coordinates gives,

$$\frac{x(\mu)}{\epsilon} \sim C e^{-2\mu/\epsilon} + \frac{\mu}{2\epsilon} - \frac{1}{4} + O(\epsilon). \quad (8)$$

The tipping point can be found when this solution (8) begins growing exponentially, so we focus on when the exponential term becomes large ($O(1/\epsilon)$),

$$e^{-2\mu/\epsilon} \sim O(1/\epsilon) \Rightarrow 2\mu \sim \epsilon \log(\epsilon). \quad (9)$$

This leads us to conclude that for small values of ϵ , the slowly varying parameter causes tipping to occur after the standard bifurcation. With this result, we compare our estimate to numerical results to evaluate it's performance for a varying size of ϵ . Qualities that show our approximation is doing well are the concavity is well represented and that as $\epsilon \rightarrow 0$ the asymptotics converge with the actual bifurcation of the system.

In figure 5 we have an example of the tipping occurring for a choice in ϵ in (a) and in (b) but it is (c) that demonstrates the tipping approximation across a range of ϵ . It is here we see an accurate concavity as well as a clear agreement of the estimation and bifurcation as $\epsilon \rightarrow 0$. Hence we may conclude that our methodology here will be useful in the Stommel case.

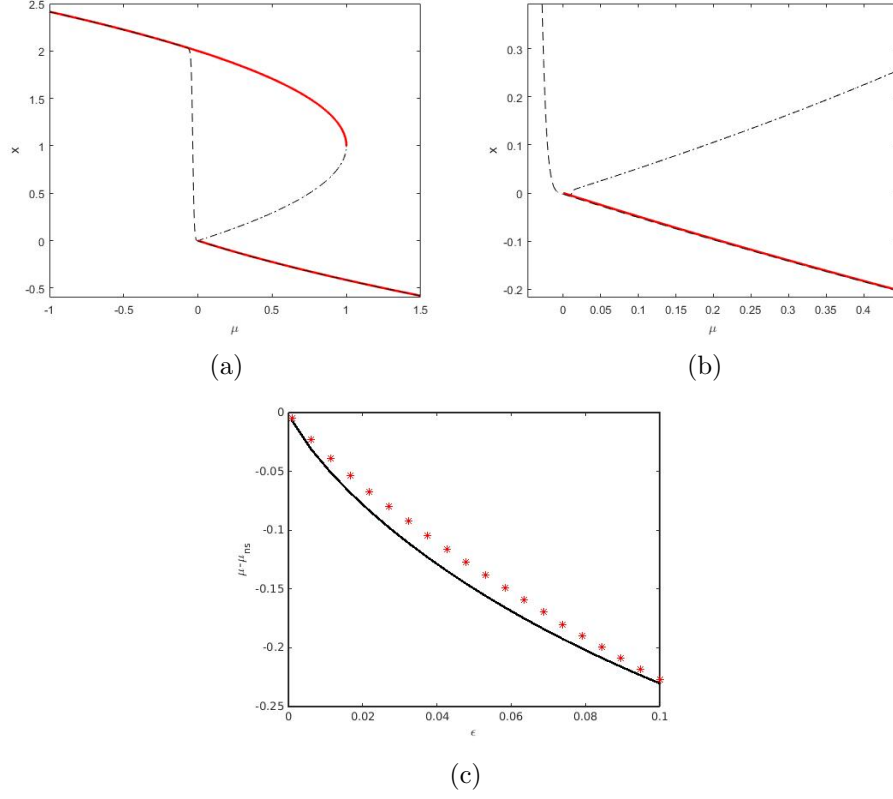


Figure 5: In (a) we have the numerical solution (black dotted line) to (3) with $A = 0$ and $\epsilon = .01$. The bifurcation plot is overlayed for convenience. In (b) we have a zoom in of what happens near the non-smooth bifurcation. The tipping occurs slightly after where the bifurcation would have occurred, here at $\mu = -.0348$ where our prediction is at $\mu = -.0230$. In (c) we have a range of ϵ and their corresponding tipping (red stars) compared to our estimate (solid black line).

High Frequency Oscillatory Forcing

Consider the system (3) with $A = O(1)$ and $\epsilon = 0$, where we have oscillatory forcing at a medium amplitude but no drifting parameter; also assume that $\Omega \gg 1$ so we have a high frequency. Where the previous section required rescaling the problem due to the slowly varying dynamics, here we have dynamics occurring on both a 'slow' time scale and a 'fast' scale. This naturally suggests a multiple scales approach where we will call our 'slow'

time $\tau = t$ and our 'fast' time $T = \Omega t$, then we search for a solution that is dependent on these scales, $x(t) = x(\tau, T)$. Introducing this method with the appropriate variable change,

$$\begin{aligned} \frac{dx}{dt} &= \frac{dx}{d\tau} \frac{d\tau}{dt} + \frac{dx}{dT} \frac{dT}{dt} = \frac{dx}{d\tau} + \Omega \frac{dx}{dT}, \\ \frac{dx}{dT} &= \Omega^{-1} \left(-\frac{dx}{d\tau} - \mu + 2|x| - x|x| + A \sin(T) \right). \end{aligned} \quad (10)$$

From this system (10), we see this small quantity, Ω^{-1} , appear which suggests the asymptotic expansion be in powers of this quantity,

$$x \sim x_0 + \Omega^{-1}x_1 + \Omega^{-2}x_2 + O(\Omega^{-3}) \quad (11)$$

Using (11) in our multiple scales system (10), we separate by orders of Ω to get,

$$\begin{aligned} O(1) : \quad x_{0T} &= 0 & &= R_0(\tau, T), \\ O(\Omega^{-1}) : \quad x_{1T} &= -x_{0\tau} - \mu + 2|x_0| - x_0|x_0| + A \sin(T) = R_1(\tau, T), \\ O(\Omega^{-2}) : \quad x_{2T} &= -x_{1\tau} - \mu + 2|x_1| - x_0|x_1| - x_1|x_0| &= R_2(\tau, T). \end{aligned}$$

Now that we have an equation on each order, we must be able to solve each one but further restrict our solution from having resonant or linearly growing terms. This will assure that the terms in the asymptotic expansion are compatible with one another and we have a robust solution.

A common method to guarantee compatible solutions on each order can be found with less than linearly growing terms is to use the Fredholm alternative which provides a solvability condition on each order,

$$\forall i \quad \lim_{T \rightarrow \infty} \frac{1}{T} \int_0^T R_i(\tau, u) du = 0.$$

We also must recall that our focus is on the non-smooth behavior and thus we restrict the solution to follow along the lower stable equilibrium branch, $x < 0$. (See appendix for an example of this work?) Applying these conditions to each order we can find the terms in (11),

$$x \sim 1 - \sqrt{1 + \mu} - \Omega^{-1}A \cos(T) + O(\Omega^{-2}). \quad (12)$$

With this expansion, we again search for when the terms reorder to see when a local analysis is needed. This occurs when $\mu \sim O(\Omega^{-1})$, and for that

range of μ the solution is also $x \sim O(\Omega^{-1})$. This leads us to the appropriate scaling for our spatial variables μ and x by Ω^{-1} in the local analysis,

$$\mu = \Omega^{-1}m, \quad x = \Omega^{-1}y.$$

Using this scaling along with the same approach as the outer region, we have an inner multiple scales system which also suggests an expansion,

$$\frac{dy}{dT} = \Omega^{-1} \left(-\frac{dy}{d\tau} - m + 2|y| \right) - \Omega^{-2}y|y| + A \sin(T), \quad (13)$$

$$y \sim y_0 + \Omega^{-1}y_1 + \Omega^{-2}y_2 + \dots \quad (14)$$

Like before, we use (14) in (13) to collect by orders of Ω ,

$$\begin{aligned} O(1) : \quad y_{0T} &= A \sin(T), \\ O(\Omega^{-1}) : \quad y_{1T} &= -t_{0\tau} - m + 2|y_0|. \end{aligned}$$

Using the Fredholm alternative to get compatible terms, the first equation here can be solved directly, $y_0 = -A \cos(T) + v_0(\tau)$. But applying the same criteria on the second equation leads to,

$$v_{0\tau} = -m + 2 \lim_{T \rightarrow \infty} \int_0^T |A \cos(u) + v_0(\tau)| du. \quad (15)$$

Here we must consider two cases of $v_0(\tau)$ that determine the difficulty of the integrand, case I: if the unknown function is large enough to keep the interior from ever changing signs and case II: if it is too small and the interior can change sign. In figure 6 we can see the behavior of each case where the solution on the right is following under case I, the first vertical line defining the boundary criteria between the cases, the middle region following under case II and the second vertical line giving the bifurcation.

Case I: $|v_0| \geq |A|$

In this case, our integral equation simplifies very nicely to a simple equation that we can use to find a stable equilibrium,

$$\frac{dv_0}{d\tau} = -m + 2|v_0| \Rightarrow v_0 = \pm \frac{m}{2}. \quad (16)$$

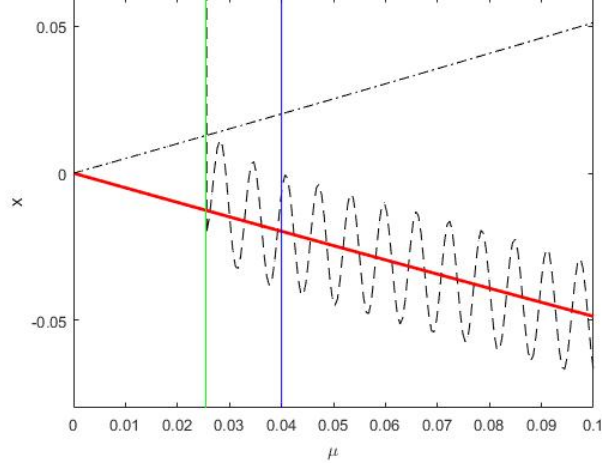


Figure 6: The asymptotic solution (black dashed line) to (3) with $A = 2$ and $\Omega = 100$. The boundary criteria (rightmost blue vertical line) here is $\mu = \frac{2|A|}{\Omega} = .04$ and the bifurcation (left green vertical line) occurs at $\mu = \frac{4|A|}{\pi\Omega} = .0255$. For reference, the original bifurcation diagram is overlaid.

Using these solutions, we can determine from a stability check that $\frac{m}{2}$ is unstable and $-\frac{m}{2}$ is stable, thus we have the leading order stable solution to our inner equation for this case which we can write in original coordinates,

$$\begin{aligned} y &\sim -\frac{m}{2} - A \cos(T) + O(\Omega^{-1}), \\ x &\sim -\frac{\mu}{2} - \Omega^{-1} A \cos(T) + O(\Omega^{-2}). \end{aligned}$$

Where the condition $|v_0| \geq |A|$ leads us to establish when this solution fails, $\mu \geq \frac{2|A|}{\Omega}$.

Case II: $|v_0| < |A|$

From case I, we have a range of μ for when this case applies, $\mu < \frac{2|A|}{\Omega}$. But the integrand in (15) is non-trivial when $|v_0| < |A|$ and from initial numerical evaluations in Fig. 7a, it is appropriate to use either quadratic or quintic interpolation to estimate the integral. We choose to use quadratic interpolation although quintic is shown in the appendix.

For quadratic interpolation, we assume that there is a function $f(v_0) =$

$a + bv_0 + cv_0^2$ and we know a few special values, $f(0) = \frac{2|A|}{\pi}$ and $f(|A|) = |A| = f(-|A|)$. From this we find,

$$f(v_0) = \frac{2|A|}{\pi} + \frac{1}{|A|} \left(1 - \frac{2}{\pi}\right) v_0^2. \quad (17)$$

In figure 7 we take a range of values in A that fall into case II, compare (17) to a Chebyshev interpolation and conclude that the approximation has sufficiently small error on $A \sim O(1)$ and hence appropriate to use in place of the integral equation (15).

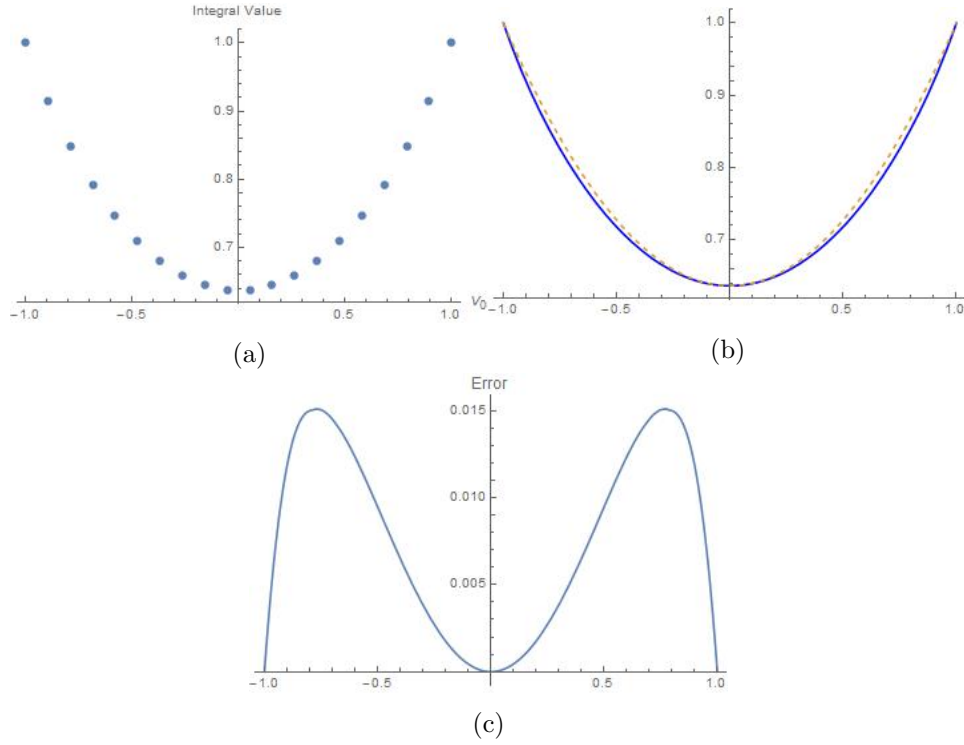


Figure 7: With a selected range of v_0 in (a), we evaluate (15). Then in (b) we fit a quadratic function (orange dotted line) and compare to a known good fit (blue solid line) via Chebyshev interpolation. Lastly, in (c) we look at the error between the curves in (b).

Thus, (15) becomes

$$\frac{dv_0}{d\tau} \approx -m + \frac{4|A|}{\pi} + \frac{2}{|A|} \left(1 - \frac{2}{\pi}\right) v_0^2. \quad (18)$$

Here we search for the equilibrium as before and find,

$$v_0 \approx \pm \sqrt{\frac{m - \frac{4|A|}{\pi}}{\frac{2}{|A|}(1 - \frac{2}{\pi})}} = \pm C \sqrt{m - \frac{4|A|}{\pi}}. \quad (19)$$

Another stability analysis leads us to choose the negative solution and this leads to the inner solution for this case,

$$\begin{aligned} y &\sim -C \sqrt{m - \frac{4|A|}{\pi}} - A \cos(T) + O(\Omega^{-1}), \\ x &\sim -C \sqrt{\frac{1}{\Omega} \left(\mu - \frac{4|A|}{\pi\Omega} \right)} - \Omega^{-1} A \cos(T) + O(\Omega^{-2}). \end{aligned}$$

It then is clear that this equilibrium fails when $\mu = \frac{4|A|}{\pi\Omega}$. From this, we can gather that the periodic forcing in the system causes the bifurcation to occur sooner. We again compare our estimate to numerical results for varying sizes of Ω^{-1} . We again look for a well represented concavity as well as convergence asymptotically for $\Omega^{-1} \rightarrow 0$ to the original bifurcation for the system.

In figure 8 we have an example of the effect oscillatory forcing has for a choice of A and Ω in (a) and (b), but in (c) we see the bifurcation approximation across a range of Ω^{-1} . There is an allowed range of Ω from our assumption, we cannot allow $\Omega \sim O(1)$ as our approximation assumed that $\Omega \gg 1$. As we can see, the concavity is well represented and the behavior as $\Omega^{-1} \rightarrow 0$ converges to the standard bifurcation. Again, this leads us to conclude that our methodology will work well in the Stommel case.

Two Dimensional Model

With the methods and approaches developed in the one dimensional model, we have at least an expectation of the behavior of the two dimensional Stommel model around the non-smooth bifurcation for differing cases. Consider the canonical model,

$$\begin{aligned} \frac{dV}{dt} &= \eta_1 - \eta_2 - V|V| - T + \eta_3(T - V), \\ \frac{dT}{dt} &= \eta_1 - T(1 + |V|), \\ \frac{d\eta_2}{dt} &= -\epsilon, \end{aligned} \quad (20)$$

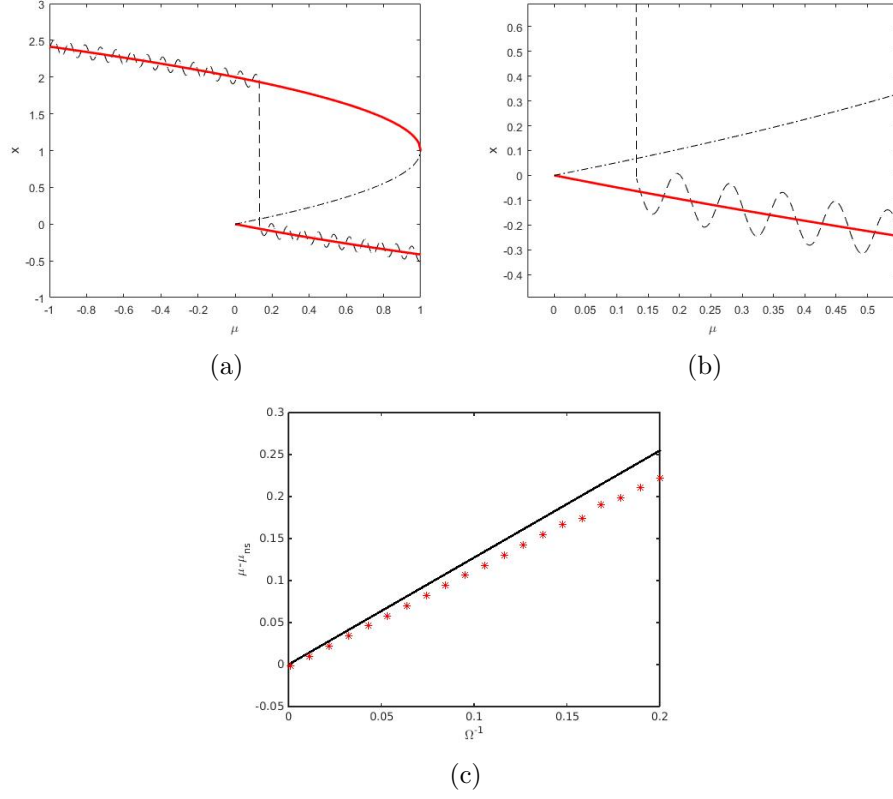


Figure 8: In (a) we have the numerical solution(black dotted line) to (3) with $A = 1$, $\Omega = 10$. In (b) we zoom in closer to the non-smooth bifurcation region. The bifurcation occurs slightly before the basic model's occurred, here at $\mu = .1314$ where our prediction is at $\mu = .1273$. In (c) we look at a range of inverse frequencies and their corresponding bifurcations (red stars) compared to our prediction (black solid line).

$$T(0) = T_i, \quad V(0) = V_i, \quad \eta_2(0) = \eta_{2i} > \eta_1 \eta_3,$$

where $0 < \epsilon \ll 1$, η_1 and η_3 are fixed positive constants. This is the Stommel model with the bifurcation parameter allowed to slowly vary. For the remainder of this section, we make the assumption that $\eta_3 < 1$ which causes (20) to admit the smooth bifurcation in the positive V region. Although not necessary, this will align our focus and give us a case to analyze in depth, the case of $\eta_3 > 1$ follows similarly.

Slowly varying η_2

Consider (20) with $\epsilon > 0$, where we allow the bifurcating parameter to slowly vary. With the choice of $\eta_3 < 1$, the lower branch with $V < 0$ is the branch we focus on in order to approach the non-smooth behavior, thus (20) becomes

$$\begin{aligned}\frac{dV}{dt} &= \eta_1 - \eta_2 + V^2 - T + \eta_3(T - V), \\ \frac{dT}{dt} &= \eta_1 - T(1 - V), \\ \frac{d\eta_2}{dt} &= -\epsilon.\end{aligned}\tag{21}$$

To begin, we immediately solve for the equilibrium of T in terms of V and write down an equation for the leading order solution for V ,

$$\begin{aligned}T(V) &= \frac{\eta_1}{1 - V}, \\ \eta_2(V_0) &= \eta_1 + V_0^2 - T(V_0) + \eta_3(T(V_0) - V_0).\end{aligned}$$

Since we know our non-smooth bifurcation to occur at $\eta_2 = \eta_1\eta_3$ when $V = 0$ and $T = \eta_1$, it makes the most sense to rescale (21) around these values. But since we couldn't form an asymptotic expansion as even the leading order term is complex, we must perform a separate analysis to determine the appropriate scaling. The resulting scaling is ϵ for each variable and this implies that the change in variable is,

$$\begin{aligned}\eta_2 &= \eta_1\eta_3 + \epsilon m, \\ V &= -\epsilon x, \\ T &= \eta_1 - \epsilon y.\end{aligned}\tag{22}$$

We introduce (22) into (21) and follow the same approach as in the one dimensional case by changing the time variable. After shifting the focus onto the parameter, we arrive at the local system with the following leading order problem,

$$\begin{aligned}\frac{dx}{dm} &= -m + \eta_3x + (1 - \eta_3)y + \epsilon x^2, \\ \frac{dy}{dm} &= -\eta_1x + y + \epsilon xy, \\ \frac{dm}{dt} &= -1,\end{aligned}\tag{23}$$

$$\begin{pmatrix} x_m \\ y_m \end{pmatrix} = \begin{pmatrix} \eta_3 & 1 - \eta_3 \\ -\eta_1 & 1 \end{pmatrix} \begin{pmatrix} x \\ y \end{pmatrix} - \begin{pmatrix} m \\ 0 \end{pmatrix}.$$

It is worthwhile to note that this leading order problem has eigenvalues that can be either real or complex depending on the choice in η_3 and η_1 .

Continuing on, we expect our tipping to occur just after the standard bifurcation from the results of the one dimensional case. But we also can expect that the same scaling will hold as we enter the $V > 0$ region, and following an identical procedure, we arrive at the system and leading order problem,

$$\begin{aligned} \frac{dx}{dm} &= -m + \eta_3 x + (1 - \eta_3)y + \epsilon x^2, \\ \frac{dy}{dm} &= \eta_1 x + y + \epsilon xy, \\ \frac{dm}{dt} &= -1, \\ \begin{pmatrix} x_m \\ y_m \end{pmatrix} &= \begin{pmatrix} \eta_3 & 1 - \eta_3 \\ \eta_1 & 1 \end{pmatrix} \begin{pmatrix} x \\ y \end{pmatrix} - \begin{pmatrix} m \\ 0 \end{pmatrix}. \end{aligned} \tag{24}$$

Which has the eigenvalues,

$$\lambda_{1,2} = \frac{\eta_3 + 1}{2} \pm \frac{1}{2} \sqrt{(1 - \eta_3)(4\eta_1 - \eta_3 + 1)}.$$

These eigenvalues must be real as $\eta_3 < 1$ guarantees the discriminant is always positive. With real eigenvalues the solution in the $V > 0$ region takes exponential form with constants $K_{i,j}$ being the j th eigenvector component corresponding to the i th eigenvalue,

$$\begin{aligned} x &\sim K_{1,1}e^{\lambda_1 m} + K_{2,1}e^{\lambda_2 m} + C_1 m + C_2, \\ y &\sim K_{1,2}e^{\lambda_1 m} + K_{2,2}e^{\lambda_2 m} + C_3 m + C_4. \end{aligned} \tag{25}$$

Translating back to our original coordinates from (25) and recalling that V contains the dynamics we are interested in,

$$\frac{V}{\epsilon} \sim K_{1,1}e^{\lambda_1(\eta_2 - \eta_1\eta_3)/\epsilon} + K_{2,1}e^{\lambda_2(\eta_2 - \eta_1\eta_3)/\epsilon} + C_1 \frac{\eta_2 - \eta_1\eta_3}{\epsilon} + C_2. \tag{26}$$

From here we have access to determining when the system is likely to tip, when one of these exponentials becomes large the system will diverge away towards the upper stable branch,

$$e^{\lambda_i(\eta_2 - \eta_1\eta_3)/\epsilon} \sim O(\epsilon^{-1}) \Rightarrow \eta_2 \sim \min\{\eta_1\eta_3 - \epsilon \ln \epsilon / \lambda_i\}, \quad i = 1, 2$$

**A note for later, for the above solution to be valid, one of the eigenvalues must be negative which introduces the restriction on the parameters,

$$\eta_1 > \frac{1}{\eta_3} - 1$$

If this restriction is not met, then the exponentials will always decay, and the analysis will then rely on the linear term.**

With a negative eigenvalue, this result again agrees with our expected delay in tipping from initial one dimensional results. We compare our estimate to numerical results for a selection of ϵ , and like before expect an accurate reflection of concavity and asymptotic convergence to the standard bifurcation as $\epsilon \rightarrow 0$.

In figure 9 we have an example of the slowly varying for a choice of ϵ in (a) and (b), but in (c) we see the tipping approximation across a range of ϵ . As expected, our prediction for tipping performs quite well by doing a decent job in replicating the concavity and converging to the static bifurcation as $\epsilon \rightarrow 0$.

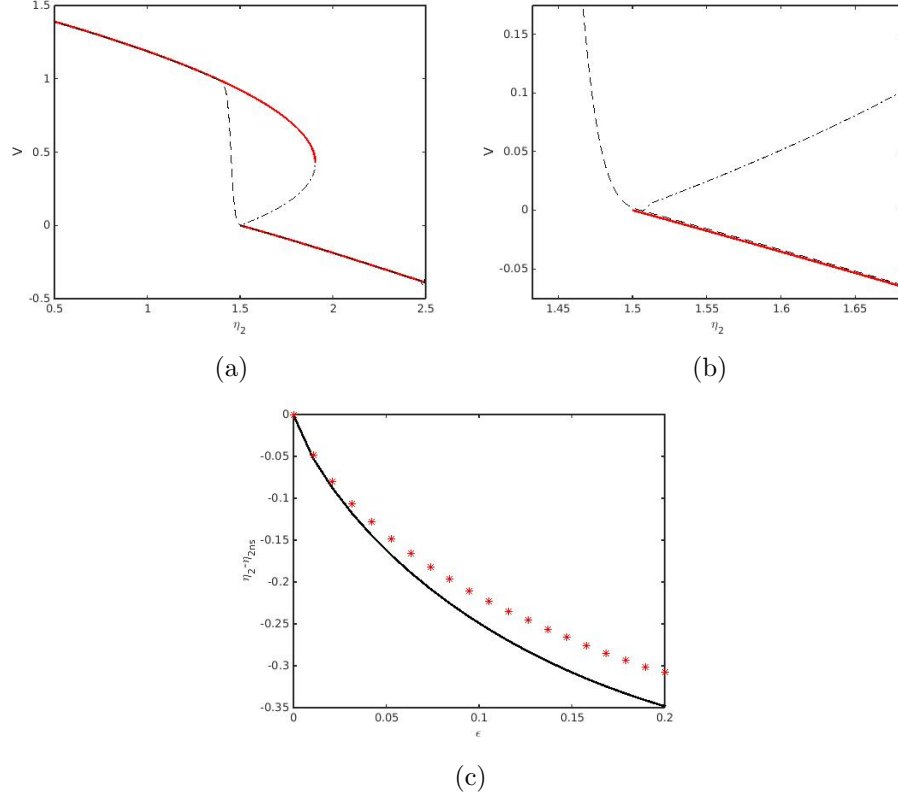


Figure 9: In (a) we have the numerical solution(black dotted line) to (20) with $\eta_1 = 4$, $\eta_3 = .375$, and $\epsilon = .01$. In (b) we zoom in closer to the non-smooth bifurcation region which occurs at $\eta_2 = 1.5$. The tipping occurs slightly after the canonical model's bifurcation occurred, $\eta_2 = 1.4502$. In (c) we look at a range of slowly varying rates and their tipping (red stars) compared to our prediction (black solid line).

Preface

You must include a preface if any part of your research was partly or wholly published in articles, was part of a collaboration, or required the approval of UBC Research Ethics Boards.

The Preface must include the following:

- A statement indicating the relative contributions of all collaborators and co-authors of publications (if any), emphasizing details of your contribution, and stating the proportion of research and writing conducted by you.
- A list of any publications arising from work presented in the dissertation, and the chapter(s) in which the work is located.
- The name of the particular UBC Research Ethics Board, and the Certificate Number(s) of the Ethics Certificate(s) obtained, if ethics approval was required for the research.

Examples

Chapter 2 is based on work conducted in UBC’s Maple Syrup Laboratory by Dr. A. Apple, Professor B. Boat, and Michael McNeil Forbes. I was responsible for tapping the trees in forests X and Z, conducted and supervised all boiling operations, and performed frequent quality control tests on the product.

A version of chapter 2 has been published [?]. I conducted all the testing and wrote most of the manuscript. The section on “Testing Implements” was originally drafted by Boat, B. Check the first pages of this chapter to see footnotes with similar information.

Note that this preface must come before the table of contents. Note also that this section “Examples” should not be listed in the table of contents, so we have used the starred form: `\section*{Example}`.

Table of Contents

Abstract	ii
Lay Summary	iii
Introduction	iv
Background	iv
Stommel Model	iv
Slowly Varying Tipping	viii
One Dimensional Model	viii
Static μ and Bifurcations	ix
Slowly varying μ	x
High Frequency Oscillatory Forcing	xii
Two Dimensional Model	xvii
Slowly varying η_2	xix
Preface	xxiii
Table of Contents	xxiv
List of Tables	xxvi
List of Figures	xxvii
List of Programs	xxix
Acknowledgements	xxx
Dedication	xxxi
1 This is a Chapter	1
1.1 A Section	1
1.1.1 This is a Subsection	1
1.2 Quote	3
1.3 Programs	3

Table of Contents

2	Another Chapter...	5
2.1	Another Section	5
2.2	Tables	6
3	Landscape Mode	9
	Bibliography	12
 Appendices		
A	First Appendix	14
B	Second Appendix	15

List of Tables

1.1	Here is the caption for this wonderful table...	2
2.1	Another table.	6
2.2	Feasible triples for highly variable Grid	7

List of Figures

1	The Stommel Two Box Model: Differing volume boxes with a temperature and salinity T_i and S_i . The boxes are connected by an overflow and capillary tube that has a flow V . There is also a surface temperature and salinity for each box T_i^s and S_i^s . We also assume well mixing occurs.	v
2	The equilibria of the non-dimensionalized system (2) with $\eta_1 = 4$ and $\eta_3 = .375$. We can see non-smooth behavior happening in both plots when $V = 0$. The red line indicates a stable branch where the dashed dotted line is for an unstable branch.	vi
3	The choice in η_3 turns out to dictate the orientation of the problem, in each plot we have fixed $\eta_1 = 4$. The case for $\eta_3 = 1$ is special due to the two bifurcations overlap and . . .	vii
4	This is the one-dimensional bifurcation diagram and we see the upper and lower equilibrium branches as well as the unstable branch. The non-smooth bifurcation occurs at (0,0) and the smooth bifurcation occurs at (1,1). Both of which are saddle-nodes due to the annihilating equilibria.	ix
5	In (a) we have the numerical solution (black dotted line) to (3) with $A = 0$ and $\epsilon = .01$. The bifurcation plot is overlaid for convenience. In (b) we have a zoom in of what happens near the non-smooth bifurcation. The tipping occurs slightly after where the bifurcation would have occurred, here at $\mu = -.0348$ where our prediction is at $\mu = -.0230$. In (c) we have a range of ϵ and their corresponding tipping (red stars) compared to our estimate (solid black line).	xii
6	The asymptotic solution (black dashed line) to (3) with $A = 2$ and $\Omega = 100$. The boundary criteria (rightmost blue vertical line) here is $\mu = \frac{2 A }{\Omega} = .04$ and the bifurcation (left green vertical line) occurs at $\mu = \frac{4 A }{\pi\Omega} = .0255$. For reference, the original bifurcation diagram is overlaid.	xv

List of Figures

- 7 With a selected range of v_0 in (a), we evaluate (15). Then in (b) we fit a quadratic function (orange dotted line) and compare to a known good fit (blue solid line) via Chebyshev interpolation. Lastly, in (c) we look at the error between the curves in (b). xvi
- 8 In (a) we have the numerical solution (black dotted line) to (3) with $A = 1$, $\Omega = 10$. In (b) we zoom in closer to the non-smooth bifurcation region. The bifurcation occurs slightly before the basic model's occurred, here at $\mu = .1314$ where our prediction is at $\mu = .1273$. In (c) we look at a range of inverse frequencies and their corresponding bifurcations (red stars) compared to our prediction (black solid line). xviii
- 9 In (a) we have the numerical solution (black dotted line) to (20) with $\eta_1 = 4$, $\eta_3 = .375$, and $\epsilon = .01$. In (b) we zoom in closer to the non-smooth bifurcation region which occurs at $\eta_2 = 1.5$. The tipping occurs slightly after the canonical model's bifurcation occurred, $\eta_2 = 1.4502$. In (c) we look at a range of slowly varying rates and their tipping (red stars) compared to our prediction (black solid line). xxii

List of Programs

- 1.1 Python program that computes the n^{th} Fibonacci number
using memoization. 4

Acknowledgements

This is the place to thank professional colleagues and people who have given you the most help during the course of your graduate work.

Dedication

The dedication is usually quite short, and is a personal rather than an academic recognition. The *Dedication* does not have to be titled, but it must appear in the table of contents. If you want to skip the chapter title but still enter it into the Table of Contents, use this command `\chapter[Dedication]{}`.

Note that this section is the last of the preliminary pages (with lowercase Roman numeral page numbers). It must be placed *before* the `\mainmatter` command. After that, Arabic numbered pages will begin.

Chapter 1

This is a Chapter

1.1 A Section

Here is a section with some text. Equations look like this $y = x$.¹
This is an example of a second paragraph in a section so you can see how much it is indented by.

1.1.1 This is a Subsection

Here is an example of a citation: [?]. The actual form of the citation is governed by the `bibliographystyle`. These citations are maintained in a BibTeX file `sample.bib`. You could type these directly into the file. For an example of the format to use look at the file `ubcsample.bbl` after you compile this file.²

This is an example of a second paragraph in a subsection so you can see how much it is indented by.

This is a Subsubsection

Here are some more citations [?, ?, ?]. If you use the `natbib` package with the `sort&compress` option, then the following citation will look the same as the first citation in this section: [?, ?, ?].

This is an example of a second paragraph in a subsubsection so you can see how much it is indented by.

This is a Paragraph Paragraphs and subparagraphs are the smallest units of text. There is no subsubsubsection etc.

¹Here is a footnote.

²Here is another footnote.

Phoenix	\$960.35
Calgary	\$250.00

Table 1.1: Here is the caption for this wonderful table. It has not been centered and the positioning has been specified to be at the top of the page. Thus it appears above the babble rather than below where it is defined in the source file.

This is a Subparagraph This is the last level of organisation. If you need more than this, you should consider reorganizing your work...

$$f(x) = \int_{-\infty}^{\infty} \int_{-\infty}^{\infty} e^{-\frac{y^2}{2}} e^{-z^2} dy dz \quad (1.1)$$

In order to show you what a separate page would look like (i.e. without a chapter heading) I must type some more text. Thus I will babble a bit and keep babbling for at least one more page... What you should notice is that the chapter titles appear substantially lower than the continuing text.

Babble babble babble babble babble babble babble babble babble babble
babble babble babble babble babble babble babble babble babble babble
babble babble babble babble babble babble babble babble babble babble
babble babble babble babble babble babble babble babble babble babble
babble.

[illegible]

1.2 Quote

Here is a quote:

This is a small poem,
a little poem, a Haiku,
to show you how to.
—Michael McNeil Forbes.

This small poem shows several features:

- The use of the `quote` and `center` environments.
- The `\newpage` command has been used to force a page break. (Sections do not usually start on a new page.)
- The `pagestyle` has been set to suppress the headers using the command `\thispagestyle{plain}`. Note that using `\pagestyle{plain}` would have affected all of the subsequent pages.

1.3 Programs

Here we give an example of a new float as defined using the `float` package. In the preamble we have used the commands

```
\floatstyle{ruled}  
\newfloat{Program}{htbp}{lop}[chapter]
```

This creates a “Program” environment that may be used for program fragments. A sample `python` program is shown in Program 1.1. (Note that Python places a fairly restrictive limit on recursion so trying to call this with a large n before building up the cache is likely to fail unless you increase the recursion depth.) Instead of using a `verbatim` environment for your program chunks, you might like to `include` them within an `alltt` environment by including the `\usepackage{alltt}` package (see page 187 of the *L^AT_EX* book). Another useful package is the `\usepackage{listings}` which can pretty-print many different types of source code.

Program 1.1 Python program that computes the n^{th} Fibonacci number using memoization.

```
def fib(n, _cache={}):
    if n < 2:
        return 1
    if n in _cache:
        return _cache[n]
    else:
        result = fib(n-1)+fib(n-2)
        _cache[n] = result
    return result
```

Chapter 2

Another Chapter with a Very Long Chapter-name that will Probably Cause Problems

This chapter name is very long and does not display properly in the running headers or in the table of contents. To deal with this, we provide a shorter version of the title as the optional argument to the `\chapter[]{}{}` command. For example, this chapter's title and associated table of contents heading and running header was created with `\chapter[Another Chapter\ldots]{Another Chapter with a Very Long Chapter-name that will Probably Cause Problems}`.

Note that, according to the thesis regulations, the heading included in the table of contents must be a truncation of the actual heading.

This Chapter was used as a demonstration in the Preface for how to attribute contribution from collaborators. If there are any such contributions, details must be included in the Preface. If you wish, you may additionally use a footnote such as this.³

2.1 Another Section

Another bunch of text to demonstrate what this file does. You might want a list for example:⁴

- An item in a list.
- Another item in a list.

³This chapter is based on work conducted in UBC's Maple Syrup Laboratory by Dr. A. Apple, Professor B. Boat, and C. Cat.

⁴Here is a footnote in a different chapter. Footnotes should come after punctuation.

An Unnumbered Section That is Not Included in the Table of Contents

Here is an example of a figure environment. Perhaps I should say that the example of a figure can be seen in Figure ???. Figure placement can be tricky with \LaTeX because figures and tables are treated as “floats”: text can flow around them, but if there is not enough space, they will appear later. To prevent figures from going too far, the `\afterpage{\clearpage}` command can be used. This makes sure that the figure are typeset at the end of the page (possibly appear on their own on the following pages) and before any subsequent text.

The `\clearpage` forces a page break so that the figure can be placed, but without the the `\afterpage{}` command, the page would be broken too early (at the `\clearpage` statement). The `\afterpage{}` command tells \LaTeX to issue the command after the present page has been rendered.

2.2 Tables

We have already included one table: 1.1. Another table is plopped right here. Well, actually, as with Figures, tables do not necessarily appear right

	Singular		Plural	
	English	Gaeilge	English	Gaeilge
1st Person	at me	agam	at us	againn
2nd Person	at you	agat	at you	agaibh
3rd Person	at him	aige	at them	acu
	at her	aici		

Table 2.1: Another table.

“here” because tables are also “floats”. \LaTeX puts them where it can. Because of this, one should refer to floats by their labels rather than by their location. This example is demonstrated by Table 2.1. This one is pretty close, however. (Note: you should generally not put tables or figures in the middle of a paragraph. This example is for demonstration purposes only.)

Another useful package is `\usepackage{longtable}` which provides the `longtable` environment. This is nice because it allows tables to span multiple pages. Table 2.2 has been formatted this way.

2.2. Tables

Table 2.2: Feasible triples for highly variable Grid

Time (s)	Triple chosen	Other feasible triples
0	(1, 11, 13725)	(1, 12, 10980), (1, 13, 8235), (2, 2, 0), (3, 1, 0)
274	(1, 12, 10980)	(1, 13, 8235), (2, 2, 0), (2, 3, 0), (3, 1, 0)
5490	(1, 12, 13725)	(2, 2, 2745), (2, 3, 0), (3, 1, 0)
8235	(1, 12, 16470)	(1, 13, 13725), (2, 2, 2745), (2, 3, 0), (3, 1, 0)
10980	(1, 12, 16470)	(1, 13, 13725), (2, 2, 2745), (2, 3, 0), (3, 1, 0)
13725	(1, 12, 16470)	(1, 13, 13725), (2, 2, 2745), (2, 3, 0), (3, 1, 0)
16470	(1, 13, 16470)	(2, 2, 2745), (2, 3, 0), (3, 1, 0)
19215	(1, 12, 16470)	(1, 13, 13725), (2, 2, 2745), (2, 3, 0), (3, 1, 0)
21960	(1, 12, 16470)	(1, 13, 13725), (2, 2, 2745), (2, 3, 0), (3, 1, 0)
24705	(1, 12, 16470)	(1, 13, 13725), (2, 2, 2745), (2, 3, 0), (3, 1, 0)
27450	(1, 12, 16470)	(1, 13, 13725), (2, 2, 2745), (2, 3, 0), (3, 1, 0)
30195	(2, 2, 2745)	(2, 3, 0), (3, 1, 0)
32940	(1, 13, 16470)	(2, 2, 2745), (2, 3, 0), (3, 1, 0)
35685	(1, 13, 13725)	(2, 2, 2745), (2, 3, 0), (3, 1, 0)
38430	(1, 13, 10980)	(2, 2, 2745), (2, 3, 0), (3, 1, 0)
41175	(1, 12, 13725)	(1, 13, 10980), (2, 2, 2745), (2, 3, 0), (3, 1, 0)
43920	(1, 13, 10980)	(2, 2, 2745), (2, 3, 0), (3, 1, 0)
46665	(2, 2, 2745)	(2, 3, 0), (3, 1, 0)
49410	(2, 2, 2745)	(2, 3, 0), (3, 1, 0)
52155	(1, 12, 16470)	(1, 13, 13725), (2, 2, 2745), (2, 3, 0), (3, 1, 0)
54900	(1, 13, 13725)	(2, 2, 2745), (2, 3, 0), (3, 1, 0)
57645	(1, 13, 13725)	(2, 2, 2745), (2, 3, 0), (3, 1, 0)
60390	(1, 12, 13725)	(2, 2, 2745), (2, 3, 0), (3, 1, 0)
63135	(1, 13, 16470)	(2, 2, 2745), (2, 3, 0), (3, 1, 0)
65880	(1, 13, 16470)	(2, 2, 2745), (2, 3, 0), (3, 1, 0)
68625	(2, 2, 2745)	(2, 3, 0), (3, 1, 0)
71370	(1, 13, 13725)	(2, 2, 2745), (2, 3, 0), (3, 1, 0)
74115	(1, 12, 13725)	(2, 2, 2745), (2, 3, 0), (3, 1, 0)
76860	(1, 13, 13725)	(2, 2, 2745), (2, 3, 0), (3, 1, 0)
79605	(1, 13, 13725)	(2, 2, 2745), (2, 3, 0), (3, 1, 0)
82350	(1, 12, 13725)	(2, 2, 2745), (2, 3, 0), (3, 1, 0)
85095	(1, 12, 13725)	(1, 13, 10980), (2, 2, 2745), (2, 3, 0), (3, 1, 0)
87840	(1, 13, 16470)	(2, 2, 2745), (2, 3, 0), (3, 1, 0)
90585	(1, 13, 16470)	(2, 2, 2745), (2, 3, 0), (3, 1, 0)
93330	(1, 13, 13725)	(2, 2, 2745), (2, 3, 0), (3, 1, 0)
Continued on next page		

Table 2.2 – continued from previous page

Time (s)	Triple chosen	Other feasible triples
96075	(1, 13, 16470)	(2, 2, 2745), (2, 3, 0), (3, 1, 0)
98820	(1, 13, 16470)	(2, 2, 2745), (2, 3, 0), (3, 1, 0)
101565	(1, 13, 13725)	(2, 2, 2745), (2, 3, 0), (3, 1, 0)
104310	(1, 13, 16470)	(2, 2, 2745), (2, 3, 0), (3, 1, 0)
107055	(1, 13, 13725)	(2, 2, 2745), (2, 3, 0), (3, 1, 0)
109800	(1, 13, 13725)	(2, 2, 2745), (2, 3, 0), (3, 1, 0)
112545	(1, 12, 16470)	(1, 13, 13725), (2, 2, 2745), (2, 3, 0), (3, 1, 0)
115290	(1, 13, 16470)	(2, 2, 2745), (2, 3, 0), (3, 1, 0)
118035	(1, 13, 13725)	(2, 2, 2745), (2, 3, 0), (3, 1, 0)
120780	(1, 13, 16470)	(2, 2, 2745), (2, 3, 0), (3, 1, 0)
123525	(1, 13, 13725)	(2, 2, 2745), (2, 3, 0), (3, 1, 0)
126270	(1, 12, 16470)	(1, 13, 13725), (2, 2, 2745), (2, 3, 0), (3, 1, 0)
129015	(2, 2, 2745)	(2, 3, 0), (3, 1, 0)
131760	(2, 2, 2745)	(2, 3, 0), (3, 1, 0)
134505	(1, 13, 16470)	(2, 2, 2745), (2, 3, 0), (3, 1, 0)
137250	(1, 13, 13725)	(2, 2, 2745), (2, 3, 0), (3, 1, 0)
139995	(2, 2, 2745)	(2, 3, 0), (3, 1, 0)
142740	(2, 2, 2745)	(2, 3, 0), (3, 1, 0)
145485	(1, 12, 16470)	(1, 13, 13725), (2, 2, 2745), (2, 3, 0), (3, 1, 0)
148230	(2, 2, 2745)	(2, 3, 0), (3, 1, 0)
150975	(1, 13, 16470)	(2, 2, 2745), (2, 3, 0), (3, 1, 0)
153720	(1, 12, 13725)	(2, 2, 2745), (2, 3, 0), (3, 1, 0)
156465	(1, 13, 13725)	(2, 2, 2745), (2, 3, 0), (3, 1, 0)
159210	(1, 13, 13725)	(2, 2, 2745), (2, 3, 0), (3, 1, 0)
161955	(1, 13, 16470)	(2, 2, 2745), (2, 3, 0), (3, 1, 0)
164700	(1, 13, 13725)	(2, 2, 2745), (2, 3, 0), (3, 1, 0)

An Unnumbered Subsection

Note that if you use subsections or further divisions under an unnumbered section, then you should make them unnumbered as well otherwise you will end up with zeros in the section numbering.

Chapter 3

Landscape Mode

The landscape mode allows you to rotate a page through 90 degrees. It is generally not a good idea to make the chapter heading landscape, but it can be useful for long tables etc.

This text should appear rotated, allowing for formatting of very wide tables etc. Note that this might only work after you convert the `dvi` file to a postscript (`ps`) or `pdf` file using `dvips` or `dvipdf` etc. This feature is provided by the `lscape` and the `pdflscape` packages. The latter is preferred if it works as it also rotates the pages in the `pdf` file for easier viewing.

[9] [4] [5] [10] [3] [1] [6] [7] [8] [2]

Bibliography

- [1] Richard B Alley, Jochem Marotzke, William D Nordhaus, Jonathan T Overpeck, Dorothy M Peteet, Roger A Pielke, RT Pierrehumbert, PB Rhines, TF Stocker, LD Talley, et al. Abrupt climate change. *science*, 299(5615):2005–2010, 2003.
- [2] David Angeli, James E Ferrell, and Eduardo D Sontag. Detection of multistability, bifurcations, and hysteresis in a large class of biological positive-feedback systems. *Proceedings of the National Academy of Sciences*, 101(7):1822–1827, 2004.
- [3] Mario Bernardo, Chris Budd, Alan Richard Champneys, and Piotr Kowalczyk. *Piecewise-smooth dynamical systems: theory and applications*, volume 163. Springer Science & Business Media, 2008.
- [4] Henk A Dijkstra. *Nonlinear climate dynamics*. Cambridge University Press, 2013.
- [5] Richard Haberman. Slowly varying jump and transition phenomena associated with algebraic bifurcation problems. *SIAM Journal on Applied Mathematics*, 37(1):69–106, 1979.
- [6] Jochem Marotzke. Abrupt climate change and thermohaline circulation: Mechanisms and predictability. *Proceedings of the National Academy of Sciences*, 97(4):1347–1350, 2000.
- [7] Stefan Rahmstorf. The thermohaline ocean circulation: A system with dangerous thresholds? *Climatic Change*, 46(3):247–256, 2000.
- [8] Stefan Rahmstorf. Ocean circulation and climate during the past 120,000 years. *Nature*, 419(6903):207–214, 2002.
- [9] Henry Stommel. Thermohaline convection with two stable regimes of flow. *Tellus*, 13(2):224–230, 1961.

- [10] Jielin Zhu, Rachel Kuske, and Thomas Erneux. Tipping points near a delayed saddle node bifurcation with periodic forcing. *SIAM journal on applied dynamical systems*, 14(4):2030–2068, 2015.

Appendix A

First Appendix

Here you can have your appendices. Note that if you only have a single appendix, you should issue `\renewcommand{\appendicesname}{Appendix}` before calling `\appendix` to display the singular “Appendix” rather than the default plural “Appendices”.

Appendix B

Second Appendix

Here is the second appendix.

Additional Information

This chapter shows you how to include additional information in your thesis, the removal of which will not affect the submission. Such material should be removed before the thesis is actually submitted.

First, the chapter is unnumbered and not included in the Table of Contents. Second, it is the last section of the thesis, so its removal will not alter any of the page numbering etc. for the previous sections. Do not include any floats, however, as these will appear in the initial lists.

The `ubcthesis` L^AT_EX class has been designed to aid you in producing a thesis that conforms to the requirements of The University of British Columbia Faculty of Graduate Studies (FoGS).

Proper use of this class and sample is highly recommended—and should produce a well formatted document that meets the FoGS requirement. Notwithstanding, complex theses may require additional formatting that may conflict with some of the requirements. We therefore *highly recommend* that you consult one of the FoGS staff for assistance and an assessment of potential problems *before* starting final draft.

While we have attempted to address most of the thesis formatting requirements in these files, they do not constitute an official set of thesis requirements. The official requirements are available at the following section of the FoGS web site:

http://www.grad.ubc.ca/current-students/dissertation-thesis-preparation

We recommend that you review these instructions carefully.